

Published in final edited form as:

*Nucl Med Biol.* 2013 October ; 40(7): 912–918. doi:10.1016/j.nucmedbio.2013.06.007.

## Whole-body pharmacokinetics of HDAC inhibitor drugs, butyric acid, valproic acid and 4-phenylbutyric acid measured with carbon-11 labeled analogs by PET

Sung Won Kim<sup>1,\*</sup>, Jacob M. Hooker<sup>2,\*</sup>, Nicola Otto<sup>3</sup>, Khaing Win<sup>4</sup>, Lisa Muench<sup>1</sup>, Colleen Shea<sup>5</sup>, Pauline Carter<sup>5</sup>, Payton King<sup>5</sup>, Alicia E. Reid<sup>6</sup>, Nora D. Volkow<sup>1,7</sup>, and Joanna S. Fowler<sup>5</sup>

<sup>1</sup>Laboratory of Neuroimaging, National Institute on Alcohol Abuse and Alcoholism, Upton, NY

<sup>2</sup>Division of Nuclear Medicine and Molecular Imaging, Massachusetts General Hospital, Harvard Medical School, Boston, MA

<sup>3</sup>Johannes-Gutenberg Universität Mainz, Institut für Organische Chemie, Duesbergweg 10-14, Mainz, Germany

<sup>4</sup>St Joseph's College, Biology and Chemistry Dept., Brooklyn, NY

<sup>5</sup>Medical Department, Brookhaven National Laboratory, Upton, NY

<sup>6</sup>Physical, Environmental and Computer Sciences, Medgar Evers College, NY

<sup>7</sup>National Institute on Drug Abuse, Bethesda, MD

### Abstract

The fatty acids, *n*-butyric acid (BA), 4-phenylbutyric acid (PBA) and valproic acid (VPA, 2-propylpentanoic acid) have been used for many years in the treatment of a variety of CNS and peripheral organ diseases including cancer. New information that these drugs alter epigenetic processes through their inhibition of histone deacetylases (HDACs) has renewed interest in their biodistribution and pharmacokinetics and the relationship of these properties to their therapeutic and side effect profile. In order to determine the pharmacokinetics and biodistribution of these drugs in primates, we synthesized their carbon-11 labeled analogues and performed dynamic positron emission tomography (PET) in six female baboons over 90 min. The carbon-11 labeled carboxylic acids were prepared by using <sup>11</sup>CO<sub>2</sub> and the appropriate Grignard reagents. [<sup>11</sup>C]BA was metabolized rapidly (only 20% of the total carbon-11 in plasma was parent compound at 5 min post injection) whereas for VPA and PBA 98% and 85% of the radioactivity was the unmetabolized compound at 30 min after their administration respectively. The brain uptake of all three carboxylic acids was very low (<0.006%ID/cc, BA>VPA>PBA), which is consistent with the need for very high doses for therapeutic efficacy. Most of the radioactivity was excreted through the kidneys and accumulated in the bladder. However, the organ biodistribution between the drugs differed. [<sup>11</sup>C]BA showed relatively high uptake in spleen and pancreas whereas [<sup>11</sup>C]PBA showed high uptake in liver and heart. Notably, [<sup>11</sup>C]VPA showed exceptionally high

\*Corresponding Authors: Sung Won Kim, PhD, Laboratory of Neuroimaging, National Institute on Alcohol Abuse and Alcoholism, Upton, NY 11973, 631-344-4398 (voice), 631-344-5815 (fax), sunny.kim@nih.gov. Jacob M. Hooker, PhD, Division of Nuclear Medicine and Molecular Imaging, Massachusetts General Hospital, Harvard Medical School, Charlestown, MA 02129, 617-726-6596 (voice), hooker@nmr.mgh.harvard.edu.

**Publisher's Disclaimer:** This is a PDF file of an unedited manuscript that has been accepted for publication. As a service to our customers we are providing this early version of the manuscript. The manuscript will undergo copyediting, typesetting, and review of the resulting proof before it is published in its final citable form. Please note that during the production process errors may be discovered which could affect the content, and all legal disclaimers that apply to the journal pertain.

heart uptake possibly due to its involvement in lipid metabolism. The unique biodistribution of each of these drugs may be of relevance in understanding their therapeutic and side effect profile including their teratogenic effects.

### Keywords

[<sup>11</sup>C]valproic acid; [<sup>11</sup>C]butyric acid; [<sup>11</sup>C]4-phenylbutyric acid; pharmacokinetics; positron emission tomography; histone deacetylase (HDAC); carbon-11

## INTRODUCTION

The fatty acids, *n*-butyric acid (BA), 4-phenylbutyric acid (PBA), and valproic acid (VPA, 2-propylpentanoic acid) shown in Fig. 1, have been used in the treatment of a variety of CNS and peripheral organ diseases including cancer (Table 1). Valproic acid (Depakote) is a widely prescribed anticonvulsant and mood stabilizing drug that is used in the treatment of epilepsy and bipolar disorder [1] with more than 7 million prescriptions in the US alone. Its mechanisms of action are not fully understood, although several have been proposed including disruption of GABAergic neurotransmission, interference of brain energy and lipid metabolism and alteration of membrane order through direct incorporation into brain lipids. VPA was also recently approved for the prophylaxis of migraine and its utility as a potential therapeutic drug for HIV in humans is being investigated [2]. Furthermore, VPA has also been used as an adjunct mood-stabilizing therapy in schizophrenia [3]. PBA (Buphenyl) has been used to treat urea cycle disorders and studies have explored its therapeutic value for sickle cell anemia [4], since increased fetal globin expression was observed in patients treated with PBA, BA [5] and VPA [6]. BA, found naturally in the colon of mammals, has been shown to be effective in reversing abnormal or transformed *in vitro* cell lines to normal functional and phenotypic states and has generated interest as a potential antitumor agent [7].

Renewed interest in these drugs has emerged because of their ability to alter gene expression through histone deacetylase (HDAC) inhibition (Table 1). HDACs remove acetyl groups from *N*-acetylated lysine residues in histones. Since DNA is wrapped around histones, histone acetylation (catalyzed by histone acetyltransferases) and deacetylation (catalyzed by HDACs) is an important process in regulating gene expression. Riggs et al. first reported HDAC inhibitory activity of BA in HeLa cells in 1977 and for more than two decades, BA was the only known HDAC inhibitor [32]. More recently, PBA and VPA were also shown to be HDAC inhibitors based on the observation of hyperacetylation of histones. This suggested the potential value of HDAC as a drug target in cancer as well as non-oncogenic diseases.

It is now recognized that many of the effects of these carboxylic acids are at least in part mediated by the inhibition of HDAC [25]. These carboxylic acid drugs as well as other HDAC inhibitors are of interest for their effects in the brain including memory enhancement and neuroprotection in rodent experiments [33] and as potential treatments of drug addiction [34]. Due to their ability to inhibit HDAC, albeit at micromolar concentrations, these three carboxylic acids and their salts have undergone phase 2 clinical trials for a variety of cancers. However, the application of these acids in cancer therapy have been limited by their low potency (requiring millimolar drug concentrations in plasma) and rapid clearance requiring continuous administration of high doses to achieve suitable plasma concentrations. The *in vivo* targets of these acids (and derivatives) as well as the molecular mechanisms of their action in disease conditions are still not well understood. Similarly, there is little information on their CNS and peripheral organ distribution and pharmacokinetics, which

may provide insight into the relationship between dosing regimens and HDAC inhibition (with chronic treatment in human) and the accumulation of the drug and/or its metabolites in brain and peripheral organs along with their potential side effects. For example, the major developmental criteria for the second generation of VPA is appropriate pharmacokinetics and biodistribution.

These gaps in knowledge have created the need to develop tools to better understand the behavior of these drugs. PET imaging, using carbon-11 radiolabeled analogues of these acids enables a noninvasive means for measuring their peripheral organ and brain penetration, pharmacokinetics and biodistribution. Such studies may provide insight into the involvement of epigenetic processes and other mechanisms in their therapeutic actions and side effects. In this article, we describe the radiosynthesis and PET imaging studies of [ $^{11}\text{C}$ ]BA [35], [ $^{11}\text{C}$ ]PBA and [ $^{11}\text{C}$ ]VPA. Each acid was radiolabeled with carbon-11 by reaction of the respective Grignard reagent with  $^{11}\text{CO}_2$  and then purified by semi-preparative HPLC. Lipophilicity (Log D at pH=7.4) and plasma protein binding (PPB) were determined following published protocols. PET imaging studies were performed using adult female baboons to obtain the distribution and kinetics of these drugs and their labeled metabolites in the brain and in peripheral organs.

## MATERIALS AND METHODS

All chemicals were obtained from Sigma Aldrich (Milwaukee, WI, USA) except for the Grignard reagents. Propyl magnesium chloride (0.5 M in THF) and phenylpropyl magnesium bromide (0.5 M in THF) were purchased from Novel Chemical Solutions (Crete, NE, USA). Sterile sodium bicarbonate solution (4.2% (wt/v)) was purchased from APP Pharmaceuticals LLC (Schaumburg, IL, USA). Anhydrous THF was prepared by distillation using sodium and benzophenone as an indicator. Radionuclide production was performed on an EBCO cyclotron (Advanced Cyclotron Systems Inc).  $^{11}\text{CO}_2$  was generated by the nuclear reaction  $^{14}\text{N}(p, \ )^{11}\text{C}$  using a gas target containing nitrogen and oxygen. Product purification was performed using a Knauer HPLC system (Sonntek Inc., Woodcliff Lake, NJ, USA) combined with NaI radioactivity detector. For semipreparative HPLC, a Phenomenex Gemini C18 column (250×10 mm, 5  $\mu\text{m}$ ) was used at a flow rate of 5 mL/min. For quality control of the radiolabeled products, analytical HPLC was performed using a Phenomenex Gemini C18 column (250×4.60 mm, 5  $\mu\text{m}$ ) at a flow rate of 1 mL/min, equipped with a Knauer HPLC system (a model K-1001 pump, a variable wavelength UV detector, a NaI radioactivity detector). HPLC mobile-phase systems consist of three sets: method A, aqueous formic acid (0.1%)/MeCN=85/15; method B, aqueous formic acid (0.1%)/MeCN=55/45; method C, aqueous formic acid (0.1%)/MeCN=50/50. Radiolabeled products were analyzed by comparison of retention times with a standard unlabeled compound by HPLC via coinjection using UV absorbance at 214 nm (BA, VPA) and 254 nm (PBA). Radiochemical purity was also determined by thin-layer chromatography (TLC) measuring radioactivity distribution on Macherey–Nagel POLYGRAM® SIL G/UV254 TLC plates with a Bioscan System 200 Imaging Scanner (Bioscan Inc., Washington, DC). All radiochemical yields are decay-corrected at the end of cyclotron bombardment.

### Synthesis of 4-Heptylmagnesium Bromide (1)

Magnesium turnings (0.203 g, 8.4 mmol) and two crystals of iodine were added to a flame-dried three-neck flask under argon atmosphere. After adding anhydrous THF (5 mL), the mixture was heated to 35°C until the suspension turned colorless. 4-Bromoheptane (1.0 g, 5.6 mmol) was dissolved in anhydrous THF (6 mL) and added dropwise at 35°C over a time period of 30 min. The reaction mixture was stirred for further 45 min and cooled to room

temperature. The Grignard reagent **1** was stored at room temperature under argon atmosphere and was used directly as precursor in the radiosynthesis.

### Radiosynthesis of [<sup>11</sup>C]Butyric Acid

At the end of bombardment (EOB), cyclotron-produced <sup>11</sup>CO<sub>2</sub> was trapped on molecular sieves 4Å (Alltech, 80–100 mesh), released in a slow stream of helium at 380 °C, and then passed through into a solution of propylmagnesium chloride in THF (0.5 M, 200 μL) at room temperature. After the measured carbon-11 radioactivity plateaued, the reaction mixture was quenched by addition of water (300 μL), followed by hydrochloric acid solution (6 N, 100 μL) and sodium hydroxide solution (6 N, 50 μL) sequentially. The mixture was diluted with HPLC eluent (H<sub>2</sub>O (0.1% formic acid)/MeCN=85:15, 1 mL), vortexed and injected into the semi-preparative reversed phase HPLC system (method A). The product was collected at the expected retention time (*t<sub>R</sub>* = 11.0 min), and the solvent was removed by rotary evaporation under reduced pressure to give decay corrected 31–50% radiochemical (specific activity, 0.2–1 Ci/μmol at EOB). In order to avoid evaporation of [<sup>11</sup>C]BA, sterile sodium bicarbonate solution (4.2% (wt/v), 0.5 mL) was added before rotary evaporation. After evaporation to dryness the product was dissolved in sterile water (4 mL) and passed through an Acrodisc® Syringe filter (0.2 μm Supor® membrane) into a sterile multi-injection vial (MIV) ready for animal study. For quality control, radiochemical purities were measured by analytical HPLC (method A, aqueous formic acid(0.1%)/MeCN=85/15; *t<sub>R</sub>* 10.5 min) and radio TLC. TLC was accomplished with the eluent (dichloromethane/MeOH=85/15) and the R<sub>f</sub> value of 0.50 for the carbon-11 labeled butyric acid, which is consistent with the unlabeled product detected by exposure of the plate to iodine vapor.

### Radiosynthesis of [<sup>11</sup>C]-4-Phenylbutyric Acid

Carbon-11 labeled 4-phenylbutyric acid was prepared according to the synthetic procedure of [<sup>11</sup>C]BA using 3-phenylpropylmagnesium bromide in THF (0.5 M, 200 μL) in a heat dried V-shaped vial at room temperature. The reaction was quenched by addition of water (300 μL), 6 M hydrochloric acid solution (100 μL) and 6 M sodium hydroxide solution (50 μL), vortexing after each addition. The mixture was diluted with HPLC eluent (H<sub>2</sub>O (0.1% formic acid)/MeCN=55:45, 1 mL), and purified by the semi-preparative reversed phase HPLC system (method B). The retention time of [<sup>11</sup>C]PBA was 11.1 min and decay corrected radiochemical yield was 40–55% (specific activity, 0.2–0.8 Ci/μmol at EOB). For radiochemical purity analysis, eluent system of radioTLC was dichloromethane/MeOH=85/15 and R<sub>f</sub> of [<sup>11</sup>C]PBA was 0.66, which is consistent with the unlabeled product.

### Radiosynthesis of [<sup>11</sup>C]Valproic Acid

[<sup>11</sup>C]VPA was prepared as described in the synthetic procedure of [<sup>11</sup>C]BA using 4-heptylmagnesium bromide as precursor. The synthesis was performed with carrier [<sup>12</sup>C]carbon dioxide gas. A heat dried V-shaped vial containing anhydrous THF (0.5 mL) was cooled to –78°C and was saturated with [<sup>12</sup>C]carbon dioxide gas. Subsequently, in a stream of helium, [<sup>11</sup>C]CO<sub>2</sub> was trapped in the THF solution. After the measured carbon-11 radioactivity peaked, 4-heptylmagnesium bromide in THF (0.5 M, 200 μL) was added into the reaction vial. The reaction mixture was heated to 45 °C for 2 minutes. The reaction mixture was quenched by addition of water (300 μL), 6 M hydrochloric acid solution (100 μL) and 6 M sodium hydroxide solution (50 μL). The mixture was diluted with HPLC eluent (H<sub>2</sub>O (0.1% formic acid)/MeCN = 50:50, 1 mL) and purified using a semipreparative reversed phase HPLC system (method C). To the collected product fraction (*t<sub>R</sub>* = 9.3 min) was added sterile sodium bicarbonate solution (4.2 % (wt/v), 0.5 mL). After evaporation to dryness the product was dissolved in sterile water (4 mL) and passed through an Acrodisc®

Syringe filter (0.2  $\mu\text{m}$  Supor® membrane) into a sterile multi-injection vial (MIV) ready for animal study. For quality control, radiochemical purities were >98% by analytical HPLC (method C;  $t_{\text{R}}$ , 8.5min) and radio TLC (eluent, dichloromethane/MeOH=85/15;  $R_{\text{f}}$ , 0.75). [ $^{11}\text{C}$ ]valproic acid was obtained in a decay-corrected radiochemical yield of 38–50%.

### Measurement of Log D and Free Fraction in Plasma

Lipophilicity at pH= 7.4 (Log D<sub>7.4</sub>) and free fraction of baboon plasma protein binding for each of the carbon-11 labeled compounds were measured according to reported procedures [36].

### PET studies in Non-Human Primates

Dynamic PET studies were performed in six female baboons in whom we imaged brain and peripheral organs. All studies were approved by the Brookhaven Institutional Animal Use and Care Committee. Baboon preparation was similar to prior studies [36]. Briefly, baboons were anesthetized with ketamine (*im*, 10 mg/Kg) and placed into the PET scanner (Siemens HR+, whole-body PET scanner; resolution, 4.5×4.5×4.8 mm at the center of field of view) for positioned to image either the brain or the thorax and abdomen. Anesthesia was maintained with a mixture of oxygen (800 mL/min), isoflurane (Forane, 1–4%) and nitrous oxide (1500 mL/min) throughout the duration of the PET scan. After acquiring a transmission scan using a  $^{68}\text{Ge}$  source, the radiotracers were injected intravenously as a bolus into the radial vein. Throughout the scan arterial blood samples were obtained from the popliteal artery to measure the total concentration of carbon-11 and the fraction present as parent carbon-11 labeled carboxylic acid in plasma. Procedures and frequency of blood sampling were performed as previously reported [36]. Briefly, plasma samples were added to either acetonitrile (0.5 mL) for [ $^{11}\text{C}$ ]VPA, or saturated ammonium sulfate (0.5 mL) solution for [ $^{11}\text{C}$ ]BA and [ $^{11}\text{C}$ ]PBA, and the resulting mixture was sonicated and centrifuged. Supernatants were spiked with the corresponding standard solution and injected onto the HPLC column (Phenomenex, Gemini C18, 250×10 mm, 5  $\mu\text{m}$ ). The radioactivity of each HPLC fraction was measured and used to determine to the percent unchanged fraction of each radiotracer. For image analysis, reconstructed PET images were analyzed by PMOD software (PMOD Technologies Ltd) to generate quantitative pharmacokinetic data.

## RESULTS AND DISCUSSION

### Radiochemistry, Log D, and PPB

Carbon-11 labeled analogues of three carboxylic acid drugs were synthesized using [ $^{11}\text{C}$ ]carbon dioxide and their corresponding Grignard reagents without the addition of carrier  $\text{CO}_2$  (no-carrier-added) for [ $^{11}\text{C}$ ]BA and [ $^{11}\text{C}$ ]PBA, and with the addition of carrier for [ $^{11}\text{C}$ ]VPA, respectively. Unlike [ $^{11}\text{C}$ ]BA and [ $^{11}\text{C}$ ]PBA, the formation of [ $^{11}\text{C}$ ]VPA required the addition of carrier  $^{12}\text{CO}_2$ . Even heating the reaction mixture to 90°C after trapping the  $^{11}\text{CO}_2$  or the use of a different solvent such as ether did not produce reaction of no-carrier-added  $^{11}\text{CO}_2$  with 4-heptylmagnesium bromide. Radiochemical yields ranged from 31–50 %, 40–55% and 38–50% for [ $^{11}\text{C}$ ]BA, [ $^{11}\text{C}$ ]PBA and [ $^{11}\text{C}$ ]VPA, respectively. The radiochemical purity measured by reversed phase HPLC and TLC were greater than 98% for all carbon-11 labeled acids. The entire process from the end of bombardment to final formulation was accomplished within 40 minutes. The lipophilicity at physiological pH was low and free fraction in plasma was variable regardless of the compound lipophilicity as shown in Table 2. The values for the percent free fraction of VPA in plasma for the baboons in this study are a little higher than those reported in a study in epilepsy patients where only 9–15% of free VPA was found after intravenous infusions [37].

### PET Studies: Plasma Analysis

The fraction of intact [ $^{11}\text{C}$ ]BA in plasma decreased rapidly to less than 20% within 5 min after injection, resulting in a very low area under the curve (AUC) compared with the two other carboxylic acid drugs (Fig. 2 and 3). Extensive metabolism and fast clearance of BA have been reported in human trials [38], suggesting that continuous iv infusion rather than oral administration seems to be the most effective method for drug administration of BA. In contrast, [ $^{11}\text{C}$ ]VPA showed the highest intact fraction in plasma (>90% over 90 min) and dose-normalized AUC, consistent with the relatively longer-half-life of VPA than that of BA and PBA. PET images reflect the presence of both the parent labeled drug and its labeled metabolites. The contribution of labeled metabolites to all carbon-11 uptake in PET images is likely to be even more significant in the liver and kidney than in other organs. However, due to relatively high fraction of carbon-11 activity present as intact VPA in plasma, we conclude that the uptake of carbon-11 in the brain and peripheral organs other than liver represents closely the pharmacokinetics of VPA.

### PET Studies: Biodistribution in Peripheral Organs

In peripheral organs, [ $^{11}\text{C}$ ]BA and [ $^{11}\text{C}$ ]PBA (and/or their labeled metabolites) showed quite different distributions (Fig. 6). [ $^{11}\text{C}$ ]BA and its labeled metabolites uptake was high in spleen and pancreas and very low in heart, while [ $^{11}\text{C}$ ]PBA uptake was high in liver and moderate in heart (Fig. 4). The excretion of [ $^{11}\text{C}$ ]PBA and/or its labeled metabolites occurred predominantly through the kidneys. [ $^{11}\text{C}$ ]BA also showed high uptake in vertebrae which was not observed for PBA nor VPA. It is notable that BA was clinically tested for the treatment of leukemia though it failed due to low bioavailability [38]. For VPA, which has been extensively used for the treatment of epilepsy, mood disorders and more recently migraine, the most recognized side effects are hepatotoxicity [39] and teratogenicity [40]. The high liver uptake of [ $^{11}\text{C}$ ]VPA is consistent with its reported extensive hepatic metabolism (Fig. 6) [41]. VPA's metabolites are considered to be responsible for its hepatotoxicity and thus its high uptake and relatively slow clearance following the initial peak and fast clearance could reflect the hepatic accumulation of these metabolites. While VPA toxicity has been attributed to its metabolites, its actions as a HDAC inhibitor are likely to contribute to its teratogenic effects, which include spina bifida, autism, cardiac, craniofacial, skeletal and limb defects. Most importantly, the heart had a remarkably high uptake of VPA, which may be due to lipid metabolism in the heart. We note that heart block and fetal heart deformities have been reported in the offspring of mothers who were given high doses of VPA during pregnancy [42]. Kaneko et al. observed placental transfer of VPA to fetus in human [43]. The extent to which epigenetic processes including HDAC inhibition may contribute to its teratogenic effects on the fetal heart merit further investigation.

### PET studies: Brain Pharmacokinetics

Low carbon-11 brain uptake ( $\sim 0.006\%$  ID/cc) was observed for [ $^{11}\text{C}$ ]BA and [ $^{11}\text{C}$ ]PBA (Fig. 7 and 8), presumably due to their anionic nature at physiological pH. *Ex vivo* rat brain analysis studies at 5 min and 30 min after [ $^{11}\text{C}$ ]BA administration showed very low intact [ $^{11}\text{C}$ ]BA fraction, indicating fast metabolism (data not shown). The brain uptake of VPA was also very low (0.004 %ID/cc), which most likely explains the very high doses needed for therapeutic efficacy (750 to 3,000 mg per day). Based on known VPA plasma concentration in therapeutic dose (50  $\mu\text{g}/\text{mL}$  to 100  $\mu\text{g}/\text{mL}$ ) [44] and brain/plasma ratio (B/P) in brain tumor patients (0.068–0.28) [45], therapeutic concentration of VPA in the brain would range between 3.4–28  $\mu\text{g}/\text{mL}$ . In our study, B/P of [ $^{11}\text{C}$ ]VPA was 0.08–0.12, which is within the reported range. However, the brain concentration is likely to be even lower considering the contribution from partial blood volume ( $\sim 5\%$  in the brain). The low brain uptake may also explain why therapeutic effects require several days of dosing since repeated dosing would result in drug accumulation in plasma including saturation of proteins

that bind it thus allowing for a higher free drug to be available to the brain [46]. Currently, even though BA, VPA, and PBA because of their HDAC inhibiting effects have generated significant interest as potential strategies for improving memory [47] and learning including its remediation in neurodegenerative diseases [48], high doses are necessary due to low brain uptake.

## CONCLUSION

Little information is available on the biodistribution and pharmacokinetics of the fatty acids, BA, PBA and VPA, though these acids have been used for many CNS and peripheral diseases and are still currently undergoing clinical trial for their second generation analogues to circumvent side effects. The PET studies in baboons presented here document the first in vivo data regarding the pharmacokinetics and whole body distribution of VPA, BA, and PBA. All three carbon-11 radiolabeled acids demonstrated poor brain uptake but varied metabolic rates and peripheral distribution. They provide new information on drug/metabolite disposition in brain and peripheral organs, which is relevant to the therapeutic and the side-effect profiles of these drugs. When considered in light of HDAC inhibition suggests that prolonged epigenetic effects (with chronic treatment in humans) may play a role in their therapeutic action. Of particular interest is the high and prolonged heart uptake of carbon-11 after the administration of VPA, which is consistent with its cardiac side effects and high heart teratogenicity during pregnancy.

## Acknowledgments

This work was performed at Brookhaven National Laboratory (BNL) with infrastructure support from the U. S. Department of Energy, Office of Biological and Environmental Research under contract DE-AC02-98CH10886. The NIH Intramural Program of the National Institute on Alcohol Abuse and Alcoholism (SWK, LM, NDV) and grant 1R01DA030321 (JMH, SWK) provided research support. Additional support was provided by the BNL Science Undergraduate Laboratory Internship Program (KW) and the Deutscher Akademischer Austauschdienst (DAAD), Bonn, Germany (NO). We thank Michael Schueller for cyclotron operations and Donald Warner for PET operations.

## References

1. Bowden CL, Swann AC, Calabrese JR, Rubenfaer LM, Wozniak PJ, Collins MA, et al. A randomized, placebo-controlled, multicenter study of divalproex sodium extended release in the treatment of acute mania. *J Clin Psychiat*. 2006; 67:1501–10.
2. Lehrman G, Hogue IB, Palmer S, Jennings C, Spina CA, Wiegand A, et al. Depletion of latent HIV-1 infection in vivo: a proof-of-concept study. *Lancet*. 2005; 366:549–55. [PubMed: 16099290]
3. Ichikawa J, Chung YC, Dai J, Meltzer HY. Valproic acid potentiates both typical and atypical antipsychotic-induced prefrontal cortical dopamine release. *Brain Res*. 2005; 1052:56–62. [PubMed: 16061211]
4. Hines P, Dover GJ, Resar LM. Pulsed-dosing with oral sodium phenylbutyrate increases hemoglobin F in a patient with sickle cell anemia. *Pediatr Blood Cancer*. 2008; 50:357–9. [PubMed: 17253639]
5. Perrine SP, Ginder GD, Faller DV, Dover GH, Ikuta T, Witkowska HE, et al. A short-term trial of butyrate to stimulate fetal-globin-gene expression in the beta-globin disorders. *N Engl J Med*. 1993; 328:81–6. [PubMed: 7677966]
6. Selby R, Nisbet-Brown E, Basran RK, Chang L, Olivieri NF. Valproic acid and augmentation of fetal hemoglobin in individuals with and without sickle cell disease. *Blood*. 1997; 90:891–3. [PubMed: 9226193]
7. Advani AS, Gibson SE, Douglas E, Jin T, Zhao X, Kalaycio M, et al. Histone H4 acetylation by immunohistochemistry and prognosis in newly diagnosed adult acute lymphoblastic leukemia (ALL) patients. *Bmc Cancer*. 2010; 10:387. [PubMed: 20663136]

8. Perrine SP, Olivieri NF, Faller DV, Vichinsky EP, Dover GJ, Ginder GD. Butyrate derivatives. New agents for stimulating fetal globin production in the beta-globin disorders. *Am J Pediatr Hematol Oncol.* 1994; 16:67–71. [PubMed: 7508690]
9. Dover GJ, Brusilow S, Samid D. Increased fetal hemoglobin in patients receiving sodium 4-phenylbutyrate. *N Engl J Med.* 1992; 327:569–70. [PubMed: 1378939]
10. Collins AF, Dover GJ, Luban NL. Increased fetal hemoglobin production in patients receiving valproic acid for epilepsy. *Blood.* 1994; 84:1690–1. [PubMed: 7520784]
11. McIntyre A, Gibson PR, Young GP. Butyrate production from dietary fibre and protection against large bowel cancer in a rat model. *Gut.* 1993; 34:386–91. [PubMed: 8386131]
12. Bourgeade MF, Cerutti I, Chany C. Enhancement of interferon antitumor action by sodium butyrate. *Cancer Res.* 1979; 39:4720–3. [PubMed: 498098]
13. Kato K, Kuhara A, Yoneda T, Inoue T, Takao T, Ohgami T, et al. Sodium butyrate inhibits the self-renewal capacity of endometrial tumor side-population cells by inducing a DNA damage response. *Mol Cancer Ther.* 2011; 10:1430–9. [PubMed: 21632462]
14. Otsuki A, Patel A, Kasai K, Suzuki M, Kurozumi K, Chiocca EA, et al. Histone deacetylase inhibitors augment antitumor efficacy of herpes-based oncolytic viruses. *Mol Ther.* 2008; 16:1546–55. [PubMed: 18648350]
15. Bhatnagar N, Li X, Chen Y, Zhou X, Garrett SH, Guo B. 3,3-Diindolylmethane enhances the efficacy of butyrate in colon cancer prevention through down-regulation of survivin. *Cancer Prev Res.* 2009; 2:581–9.
16. Rudek MA, Zhao M, He P, Hartke C, Gilbert J, Gore SD, et al. Pharmacokinetics of 5-azacitidine administered with phenylbutyrate in patients with refractory solid tumors or hematologic malignancies. *J Clin Oncol.* 2005; 23:3906–11. [PubMed: 15851763]
17. Chang JG, Hsieh-Li HM, Jong YJ, Wang NM, Tsai CH, Li H. Treatment of spinal muscular atrophy by sodium butyrate. *Proc Natl Acad Sci.* 2001; 98:9808–13. [PubMed: 11504946]
18. Chung YL, Pui NN. Phenylbutyrate suppresses distinct skin reactions that are enhanced by blockade of epidermal growth factor receptor signaling. *J Dermatol Sci.* 2011; 64:163–73. [PubMed: 21924869]
19. Michaelis M, Suhan T, Cinatl J, Driever PH, Cinatl J Jr. Valproic acid and interferon-alpha synergistically inhibit neuroblastoma cell growth in vitro and in vivo. *Int J Oncol.* 2004; 25:1795–9. [PubMed: 15547719]
20. Schroeder FA, Lin CL, Crusio WE, Akbarian S. Antidepressant-like effects of the histone deacetylase inhibitor, sodium butyrate, in the mouse. *Biol Psychiatry.* 2007; 62:55–64. [PubMed: 16945350]
21. Govindarajan N, Agis-Balboa RC, Walter J, Sananbenesi F, Fischer A. Sodium butyrate improves memory function in an Alzheimer's disease mouse model when administered at an advanced stage of disease progression. *J Alzheimers Dis.* 2011; 26:187–97. [PubMed: 21593570]
22. Cudkowicz ME, Andres PL, Macdonald SA, Bedlack RS, Choudry R, Brown RH Jr, et al. Phase 2 study of sodium phenylbutyrate in ALS. *Amyotroph Lateral Sc.* 2009; 10:99–106.
23. Wadman RI, Bosboom WM, van den Berg LH, Wokke JH, Iannaccone ST, Vrancken AF. Drug treatment for spinal muscular atrophy types II and III. *Cochrane Database Syst Rev.* 2011; 12:CD006282. [PubMed: 22161400]
24. Romieu P, Deschattrettes E, Host L, Gobaille S, Sandner G, Zwiller J. The inhibition of histone deacetylases reduces the reinstatement of cocaine-seeking behavior in rats. *Curr Neuropharmacol.* 2011; 9:21–5. [PubMed: 21886555]
25. Ricobaraza A, Cuadrado-Tejedor M, Perez-Mediavilla A, Frechilla D, Del Rio J, Garcia-Osta A. Phenylbutyrate ameliorates cognitive deficit and reduces tau pathology in an Alzheimer's disease mouse model. *Neuropsychopharmacology.* 2009; 34:1721–32. [PubMed: 19145227]
26. Chiu C-T, Liu G, Leeds P, Chuang D-M. Combined treatment with the mood stabilizers lithium and valproate produces multiple beneficial effects in transgenic mouse models of huntington's disease. *Neuropsychopharmacology.* 2011; 36:2406–21. [PubMed: 21796107]
27. Anderson GD, Temkin NR, Awan AB, Winn HR. Effect of time, injury, age and ethanol on interpatient variability in valproic acid pharmacokinetics after traumatic brain injury. *Clin Pharmacokinet.* 2007; 46:307–18. [PubMed: 17375982]

28. Gill D, Derry S, Wiffen PJ, Moore RA. Valproic acid and sodium valproate for neuropathic pain and fibromyalgia in adults. *Cochrane Database Syst Rev.* 2011:CD009183. [PubMed: 21975791]
29. Hamer HM, Jonkers DM, Vanhoutvin SA, Troost FJ, Rijkers G, de Bruine A, et al. Effect of butyrate enemas on inflammation and antioxidant status in the colonic mucosa of patients with ulcerative colitis in remission. *Clin Nutr.* 2010; 29:738–44. [PubMed: 20471725]
30. Scheppach W, Sommer H, Kirchner T, Paganelli GM, Bartram P, Christl S, et al. Effect of butyrate enemas on the colonic mucosa in distal ulcerative colitis. *Gastroenterology.* 1992; 103:51–6. [PubMed: 1612357]
31. Khan N, Jeffers M, Kumar S, Hackett C, Boldog F, Khramtsov N, et al. Determination of the class and isoform selectivity of small-molecule histone deacetylase inhibitors. *Biochem J.* 2008; 409:581–9. [PubMed: 17868033]
32. Boffa LC, Vidali G, Mann RS, Allfrey VG. Suppression of histone deacetylation in vivo and in vitro by sodium butyrate. *J Biol Chem.* 1978; 253:3364–6. [PubMed: 649576]
33. Reolon GK, Maurmann N, Werenicz A, Garcia VA, Schroder N, Wood MA, et al. Posttraining systemic administration of the histone deacetylase inhibitor sodium butyrate ameliorates aging-related memory decline in rats. *Behav Brain Res.* 2011; 221:329–32. [PubMed: 21421011]
34. Bernabeu R, Pastor V, Host L, Zwiller J. Histone deacetylase inhibition decreases preference without affecting aversion for nicotine. *J Neurochem.* 2011; 116:636–45. [PubMed: 21166804]
35. Neu H, Kihlberg T, Langstrom B. Synthesis of saturated fatty acids C-11 (C-13)-labelled in the omega-methyl position. *J Labelled Compd Rad.* 1997; 39:509–24.
36. Kim SW, Biegon A, Katsamanis ZE, Ehrlich CW, Hooker JM, Shea C, et al. Reinvestigation of the synthesis and evaluation of N-methyl-(11)C vorozole, a radiotracer targeting cytochrome P450 aromatase. *Nucl Med Bio.* 2009; 36:323–34. [PubMed: 19324278]
37. Cloyd JC, Dutta S, Cao G, Walch JK, Collins SD, Granneman GR. Valproate unbound fraction and distribution volume following rapid infusions in patients with epilepsy. *Epilepsy Res.* 2003; 53:19–27. [PubMed: 12576164]
38. Miller AA, Kurschel E, Osieka R, Schmidt CG. Clinical pharmacology of sodium-butyrate in patients with acute-leukemia. *Eur J Cancer Clin Oncol.* 1987; 23:1283–7. [PubMed: 3678322]
39. Koenig SA, Buesing D, Longin E, Oehring R, Hauessermann P, Kluger G, et al. Valproic acid-induced hepatopathy: Nine new fatalities in Germany from 1994 to 2003. *Epilepsia.* 2006; 47:2027–31. [PubMed: 17201699]
40. Ornoy A. Valproic acid in pregnancy: How much are we endangering the embryo and fetus? *Reprod. Toxicol.* 2009; 28:1–10.
41. Silva MFB, Aires CCP, Luis PBM, Ruiter JPN, Ijst L, Duran M, et al. Valproic acid metabolism and its effects on mitochondrial fatty acid oxidation: A review. *J Inherit Metab Dis.* 2008; 31:205–16. [PubMed: 18392741]
42. Sodhi P, Poddar B, Parmar V. Fatal cardiac malformation in fetal valproate syndrome. *Indian J Pediatrics.* 2001; 68:989–90.
43. Kaneko S, Otani K, Fukushima Y, Sato T, Nomura Y, Ogawa Y. Trans-placental passage and half-life of sodium valproate in infants born to epileptic mothers. *Br J Clin Pharmacol.* 1983; 15:503–6. [PubMed: 6405774]
44. Turnbull DM, Rawlins MD, Weightman D, Chadwick DW. Plasma concentrations of sodium valproate - their clinical value. *Ann Neurol.* 1983; 14:38–42. [PubMed: 6412620]
45. Vajda FJE, Donnan GA, Phillips J, Bladin PF. Human-brain, plasma, and cerebrospinal-fluid concentration of sodium valproate after 72 hours of therapy. *Neurology.* 1981; 31:486–7. [PubMed: 6783980]
46. Yu HY, Shen YZ. Dose-dependent inhibition in plasma-protein binding of valproic acid during continued treatment in guinea-pigs. *J Pharm Pharmacol.* 1992; 44:408–12. [PubMed: 1359055]
47. Fischer A, Sananbenesi F, Wang XY, Dobbin M, Tsai LH. Recovery of learning and memory is associated with chromatin remodelling. *Nature.* 2007; 447:178–U2. [PubMed: 17468743]
48. Guan JS, Haggarty SJ, Giacometti E, Dannenberg JH, Joseph N, Gao J, et al. HDAC2 negatively regulates memory formation and synaptic plasticity. *Nature.* 2009; 459:55–U8. [PubMed: 19424149]

49. Burkitt K, Ljungman M. Phenylbutyrate interferes with the Fanconi anemia and BRCA pathway and sensitizes head and neck cancer cells to cisplatin. *Mol Cancer*. 2008; 7:24. [PubMed: 18325101]
50. Collins AF, Pearson HA, Giardina P, McDonagh KT, Brusilow SW, Dover GJ. Oral sodium phenylbutyrate therapy in homozygous beta thalassemia: a clinical trial. *Blood*. 1995; 85:43–9. [PubMed: 7528572]
51. Dover GJ, Brusilow S, Charache S. Induction of fetal hemoglobin production in subjects with sickle cell anemia by oral sodium phenylbutyrate. *Blood*. 1994; 84:339–43. [PubMed: 7517215]
52. Resar LM, Segal JB, Fitzpatrick LK, Friedmann A, Brusilow SW, Dover GJ. Induction of fetal hemoglobin synthesis in children with sickle cell anemia on low-dose oral sodium phenylbutyrate therapy. *J Pediatr Hematol Oncol*. 2002; 24:737–41. [PubMed: 12468915]
53. Kuendgen A, Schmid M, Schlenk R, Knipp S, Hildebrandt B, Steidl C, et al. The histone deacetylase (HDAC) inhibitor valproic acid as monotherapy or in combination with all-trans retinoic acid in patients with acute myeloid leukemia. *Cancer*. 2006; 106:112–9. [PubMed: 16323176]
54. Masoudi A, Elopore M, Amini E, Nagel ME, Ater JL, Gopalakrishnan V, et al. Influence of valproic acid on outcome of high-grade gliomas in children. *Anticancer Res*. 2008; 28:2437–42. [PubMed: 18751431]
55. Adolf GR, Swetly P. Effects of butyrate on induction and action of interferon. *Biochem Biophys Res Commun*. 1981; 103:806–12. [PubMed: 6174120]
56. VanValkenburg C, Kluznik JC, Merrill R. New uses of anticonvulsant drugs in psychosis. *Drugs*. 1992; 44:326–35. [PubMed: 1382932]
57. Butzner JD, Parmar R, Bell CJ, Dalal V. Butyrate enema therapy stimulates mucosal repair in experimental colitis in the rat. *Gut*. 1996; 38:568–73. [PubMed: 8707089]
58. Segain JP, Raingeard de la Bletiere D, Bourreille A, Leray V, Gervois N, Rosales C, et al. Butyrate inhibits inflammatory responses through NFkappaB inhibition: implications for Crohn's disease. *Gut*. 2000; 47:397–403. [PubMed: 10940278]
59. Srinivasan K, Sharma SS. Sodium phenylbutyrate ameliorates focal cerebral ischemic/reperfusion injury associated with comorbid type 2 diabetes by reducing endoplasmic reticulum stress and DNA fragmentation. *Behav Brain Res*. 2011; 225:110–6. [PubMed: 21767572]

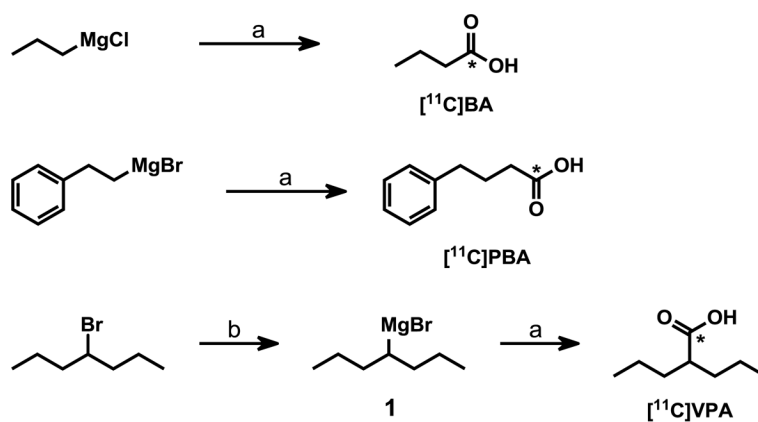


**FIG. 1.** Synthesis scheme of C-11 labeled of butyric acid (BA), valproic acid (VPA), 4-phenylbutyric acid (PBA). (a)  $^{11}\text{C}\text{CO}_2$ ; (b) Mg/THF; \*, carbon-11 labeled carbon.

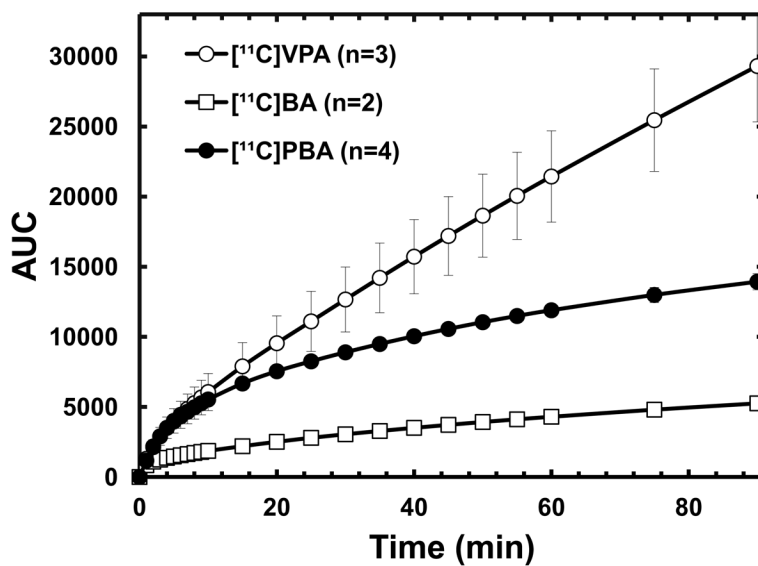


**FIG. 2.** The time–AUC plots of averaged non-metabolized carbon-11 labeled carboxylic acids in baboon plasma. [ $^{11}\text{C}$ ]VPA, open circle; [ $^{11}\text{C}$ ]BA, open rectangle; [ $^{11}\text{C}$ ]PBA, closed circle.

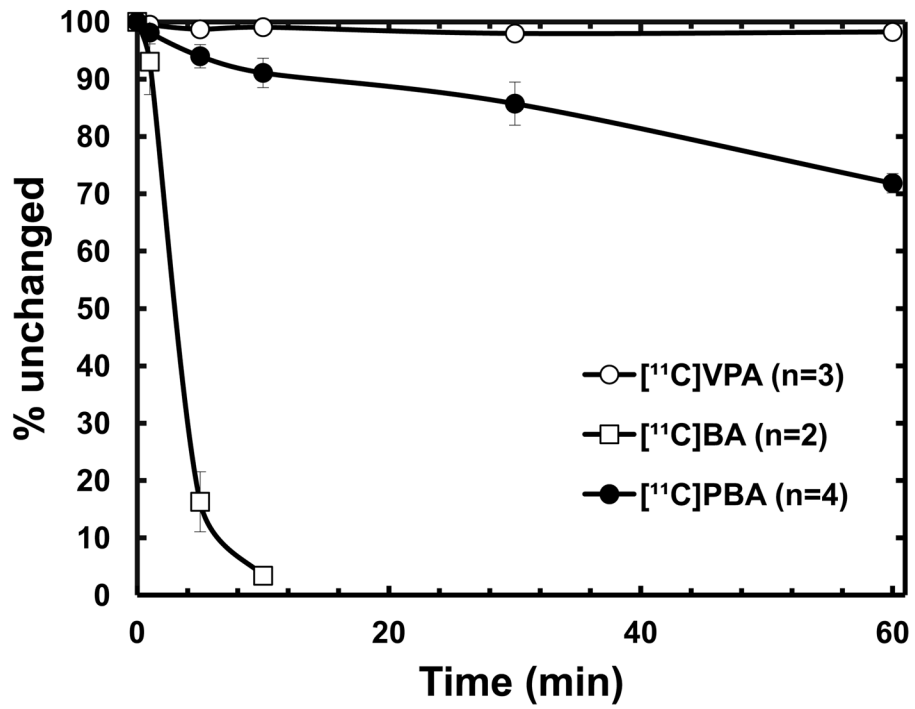


**FIG. 3.** The percentage of unchanged carbon-11 labeled carboxylic acids in baboon plasma. [<sup>11</sup>C]VPA, open circle; [<sup>11</sup>C]BA, open rectangle; [<sup>11</sup>C]PBA, closed circle.

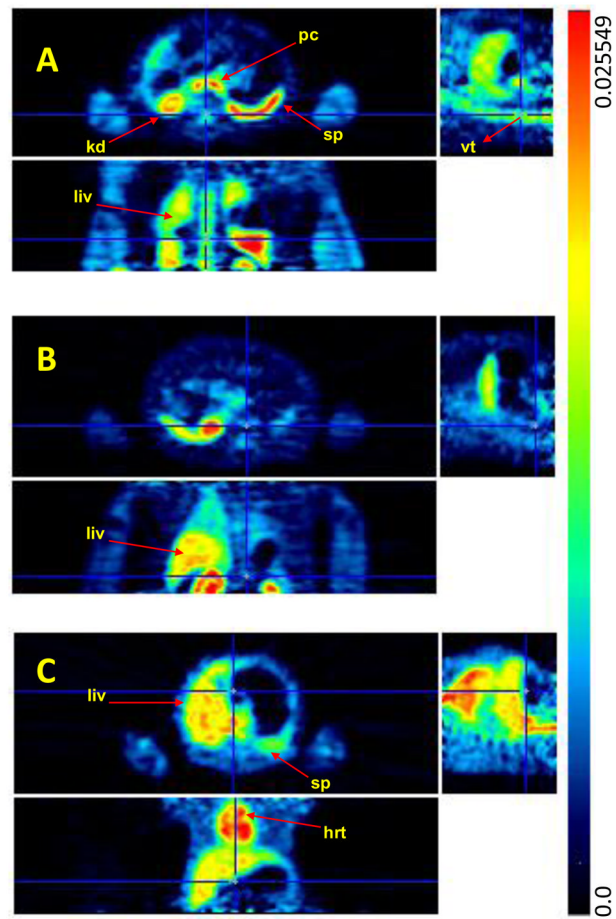


**FIG. 4.** PET images of [ $^{11}\text{C}$ ]BA (A), [ $^{11}\text{C}$ ]PBA (B), and [ $^{11}\text{C}$ ]VPA (C) (averaged %ID/cc over 30 min –90 min after iv injection) at the level of the thorax and the abdomen. The images in the top, bottom, and right row correspond to the transaxial, coronal and sagittal planes, respectively. Arrows point to the pancreas (pc), kidneys (k), spleen (sp), liver (liv), vertebrae (vt), and heart (hrt).

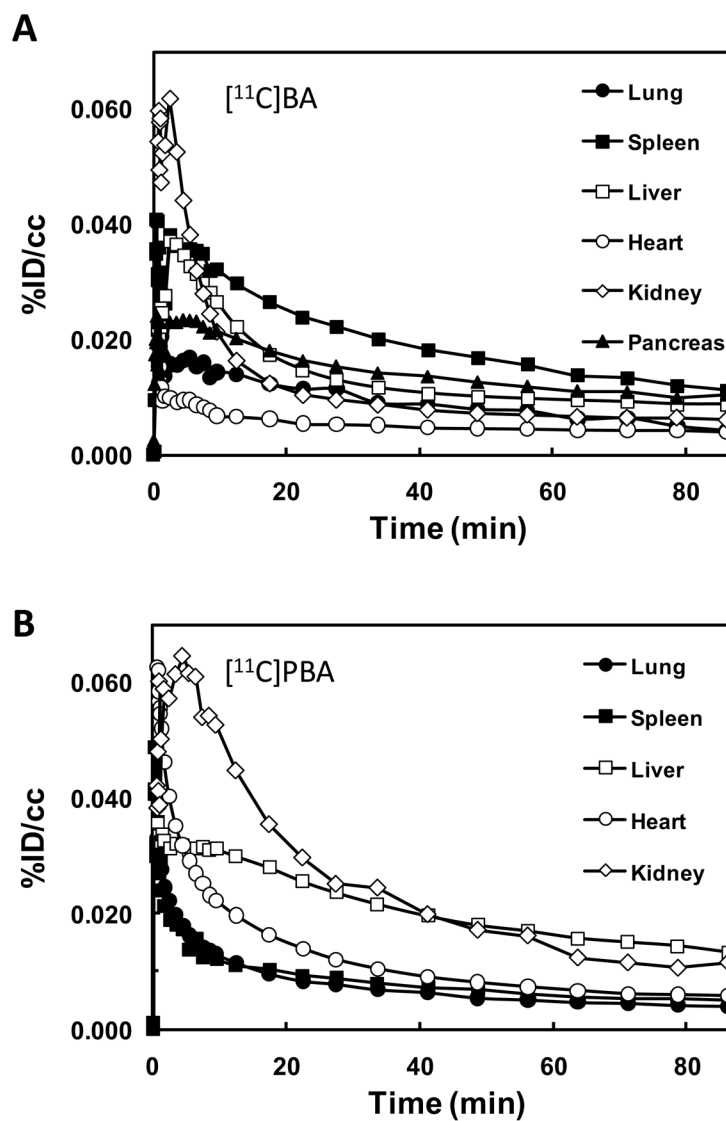


**FIG. 5.** Time-activity curves of [<sup>11</sup>C]BA (A) and [<sup>11</sup>C]PBA (B) in peripheral organs

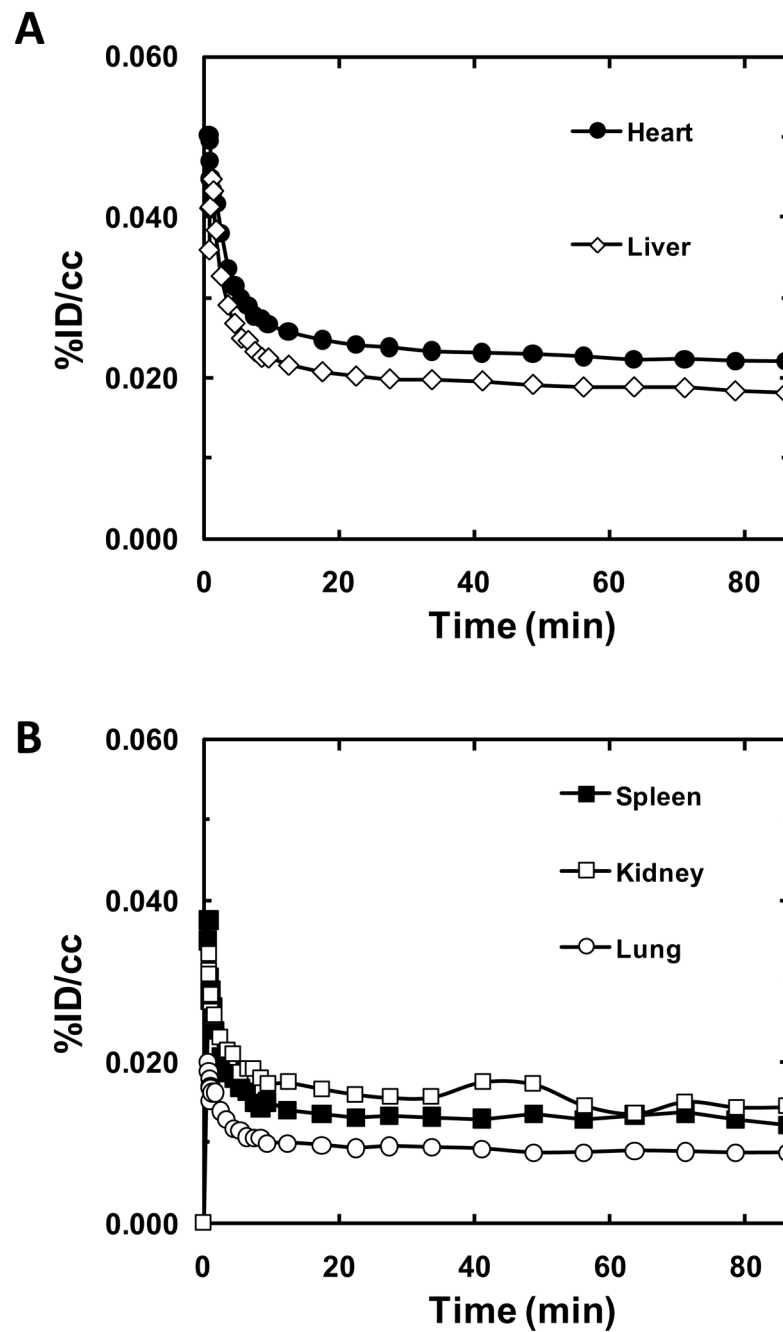


**FIG. 6.**  
Time-activity curves of [<sup>11</sup>C]VPA in peripheral organs.

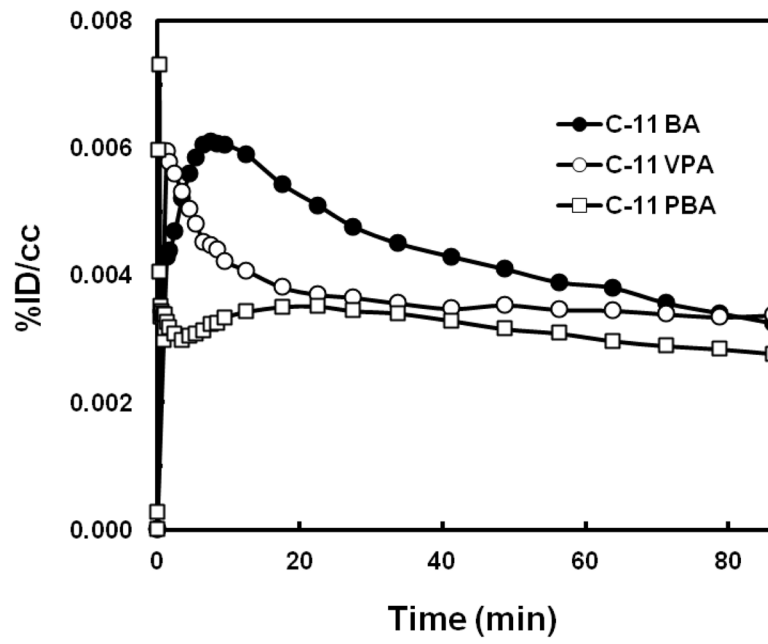


**FIG. 7.** Time-activity curves of the three carbon-11 labeled carboxylic acids in the baboon brain. BA, butyric acid; PBA, 4-phenylbutyric acid; VPA, valproic acid.

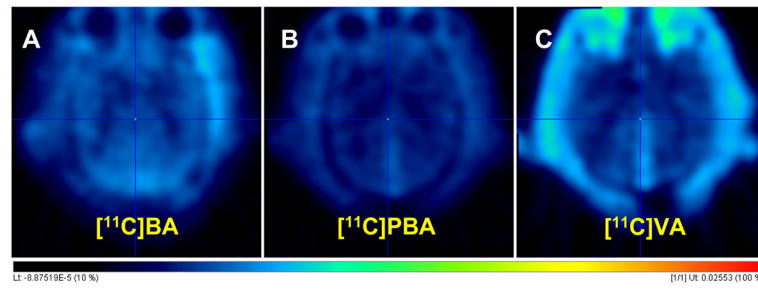


**FIG. 8.** The PET images averages over 90 min for the brain for  $[^{11}\text{C}]\text{BA}$  (A),  $[^{11}\text{C}]\text{PBA}$  (B) and  $[^{11}\text{C}]\text{VPA}$  (C). Dose-normalized images (%ID/cc) in the Transaxial view.

**Table 1**

Publications on BA, PBA, VA related to HDAC in human diseases.

Disease/Process	Relevance	BA	PBA	VPA
Anemias	HDAC inhibition stimulates fetal hemoglobin (HbF) production (particularly relevant to sickle cell anemia).	h [5, 8]; r [11]	h [9]	h [6, 10]
Cancer	HDAC inhibitors increase the sensitivity of many types of cancer to traditional chemotherapeutics.	m [12–14]	h [15, 16];	h [17]
immune modulation	HDAC inhibition appears to exhibit anti-inflammatory properties, reducing the activation of the NF- $\kappa$ B cascade and inhibiting the production of inflammatory cytokines.	m [7, 12]	m [18]	m [19]
neurological/psychiatric	HDAC inhibitors have been tested for psychiatric illness treatment; they exhibit neuroprotective properties. HDAC inhibition has reversed symptoms in animal models of Alzheimer's, ALS, and muscle atrophy. HDAC inhibitors have been shown to reduce the severity of neuropathic pain and they have also been shown to enhance memory and learning in laboratory animals.	m [20] m [21]	h [22, 23]; r [24]; m [25]	m [26]; h [27, 28]
Others	Inflammatory bowel disease (BA), diabetes (PBA), HIV (VPA)	h [29, 30];	h [31];	h [2]

Abbreviations: h (human); r (rat); m (mouse); BA (butyric acid); PBA (phenylbutyric acid); VPA (valproic acid).

**Table 2**Comparison of log D and free fraction in plasma for [<sup>11</sup>C]BA, [<sup>11</sup>C]VPA [<sup>11</sup>C]PBA.

<b>Radioligands</b>	<b>M.W.</b>	<b>Log D at pH 7.4</b>	<b>% unbound in plasma</b>
[ <sup>11</sup> C]BA	88.1	1.02±0.08 (n=3)	82±0.4 (n=2)
[ <sup>11</sup> C]PBA	164.2	-0.20±0.03 (n=6)	1.5±0.7 (n=6)
[ <sup>11</sup> C]VPA	144.2	0.26±0.03 (n=5)	26±0.3 (n=2)